

Chapter 1

OVERVIEW OF LUMINESCENCE SIGNALS FROM DOSIMETRIC MATERIALS

Abstract In this introductory chapter we introduce several models for analyzing thermally stimulated luminescence signals, which are commonly used for luminescence dosimetry and luminescence dating. We provide an overview and mathematical description of commonly used luminescence models for Thermoluminescence (TL), based on delocalized transitions involving the conduction/valence bands in solids.

1.1 Introduction

In this introductory section we provide an overview of the chapter, and of thermally stimulated luminescence signals.

When a solid is irradiated, the irradiation process ionizes the atoms and creates electrons in the conduction band and holes in the valence band. The electrons from the conduction band are trapped in electron traps and the holes in hole traps (which can also act as luminescence centers) within the forbidden band. After irradiation the system is in an excited state, and the lifetime of these excited states in nature varies widely from microseconds to billions of years. When the material is thermally stimulated in the laboratory, the trapped electrons are released and may eventually recombine with holes at luminescence centers, thus causing the emission of light from the sample. This is the origin of thermoluminescence (TL) signals, which are used widely in luminescence dosimetry and luminescence dating.

Sect.1.2 provides a general describes of the irradiation process in solids, and the creation or annihilation of electron traps, hole traps and recombination centers.

Various stimulation methods are commonly used in the laboratory to liberate the trapped electrons, and these methods generate different stimulated luminescence (SL) signals. In terms of the time scales involved in luminescence processes, one can distinguish two broad types of experiments. In the first

2.1 OVERVIEW OF LUMINESCENCE SIGNALS FROM DOSIMETRIC MATERIALS

category one studies phenomena like thermoluminescence (TL), isothermal luminescence (ITL), optically stimulated luminescence (OSL) and infrared stimulated luminescence (IRSL), which take place in time scales of seconds.

A general description of TL and ITL signals is given in Sect.1.3 and Sect.1.4 respectively. An overview of OSL and IRSL signals measured with visible and infrared light are presented in Sect.1.5 and Sect.1.6.

In the second category of time-resolved (TR) experiments, one uses short light pulses to separate the stimulation and emission of luminescence in time. TR experiments usually involve much shorter time scales than TL/OSL, typically of the order of milliseconds or microseconds. An overview of TR signals is given in Sect.1.7 of this chapter. The chapter continues in Sect.1.8, with a brief description of optical absorption (OA) and Electron Spin Resonance signals (ESR), and their connection and importance in luminescence dosimetry.

An brief summary of electron spin resonance (ESR) and optical absorption (OA) experiments, and their correlation with luminescence signals is given in Sect.1.8. Finally, the chapter concludes in Sect.1.9, with a general of what types of information researchers can obtain from the analysis of luminescence signals from dosimetric materials.

For a comprehensive review of the phenomena described in this book, the readers are directed to several available textbooks and review articles on luminescence dosimetry and its applications (Chen and Pagonis [31], Yukihara and McKeever [161], Pagonis et al. [107], Böetter-Jensen et al. [11], Chen and McKeever [30]). For a recent comprehensive review of several TL models and their analytical solutions, the reader is referred to the review article by Kitis et al. [75]. For a recent extensive compilation of R codes describing luminescence phenomena, the reader is referred to the book by Pagonis [94].

1.2 Irradiation of solids: Electron traps, Hole traps and Recombination centers

The interaction of ionizing radiation with both natural and artificial inorganic materials makes these materials suitable to act as radiation detectors. An important family of radiation detectors, called passive detectors, is based on the existence of localized energy levels within the forbidden energy band. These energy levels are created by the presence of imperfections and impurities in the crystal lattice, and by the irradiation of these materials in nature or in the laboratory.

In the framework of the energy band model of solids, the irradiation process creates electrons in the conduction band and holes in the valence band. The electrons from the conduction band are trapped in *electron traps*, and the holes are trapped in *hole traps*, represented by energy levels within the

forbidden band. The electron and hole traps can also act as *luminescence centers*.

Figure 1.1a shows a schematic example of trapping of electrons and holes in a natural crystal. In this example, the interaction of ionizing radiation with the crystalline lattice creates and mobilizes simultaneously a valence electron (shown as a black dot), and the corresponding hole (shown as a red dot). The produced electron and hole represent free charges which migrate through the crystal, until they are eventually captured at oppositely-charged lattice defects, as shown in Fig.1.1b. The electrons would be captured at positively charged electron traps (shown as a light green circle), while the holes can be captured in negatively charged hole traps (shown as a shaded gray circle).

After irradiation the system is in an excited state, and the lifetime of these excited states in nature varies widely from microseconds to billions of years. When the material is thermally or optically stimulated in the laboratory, the trapped electrons are released and may eventually recombine with holes at luminescence centers, thus causing the emission of light from the sample. Figure 1.1b shows schematically this recombination process. By applying for example heat to the crystal in the laboratory, the trapped electron (or hole) becomes mobile and recombines with the trapped hole, releasing energy in the form of a photon.

The property making the material a dosimeter is the functional relationship between the number of electrons trapped in the material and the irradiation dose.

All real crystals are not ideal, in the sense that they always include imperfections, namely *defects* and *impurities*. These imperfections cause a local change in the periodicity of the crystal, and new energy levels are thus produced within the forbidden energy band gap, which makes it possible for electrons and holes to get trapped (Chen and Pagonis [31]).

A well known defect type is the *Frenkel defects* which are interstitial atoms, ions or molecules normally located on the lattice site, which have moved out of their original place in the crystal, as shown schematically by the arrow in Fig.1.2a. The corresponding vacancies are called *Schottky defects* and are shown schematically by the squares in Fig.1.2b. Schottky defects could be created, for example, by the diffusion of the host ions to the surface of the crystal.

4.1 OVERVIEW OF LUMINESCENCE SIGNALS FROM DOSIMETRIC MATERIALS

TRAPPING AND DETRAPPING OF ELECTRONS IN A CRYSTAL

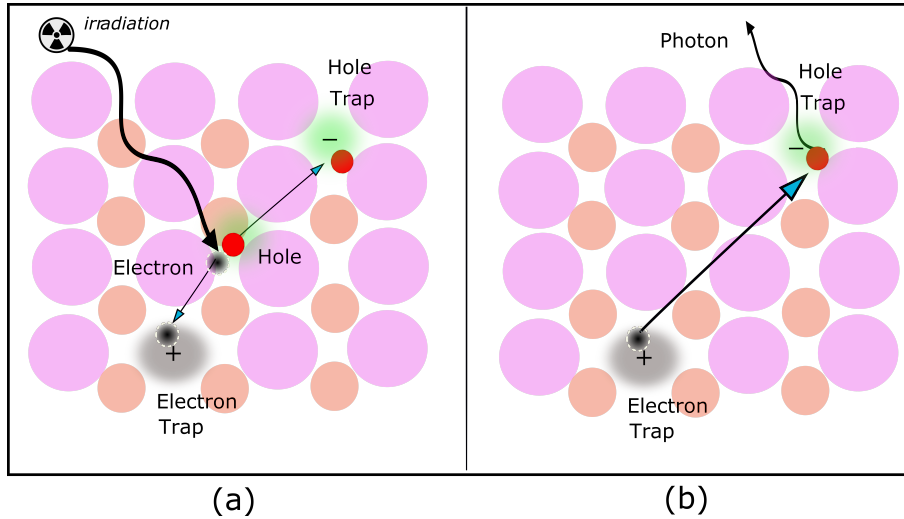


Fig. 1.1: Trapping and detrapping of electrons in a natural crystal. (a) Ionizing radiation creates mobile electron hole pairs, which can migrate through the crystal, until they are captured in oppositely-charged lattice defects. (b) Thermal or optical excitation of the crystal releases the trapped electron and it recombines with a trapped hole, releasing a photon.

FRENKEL AND SCHOTTKY DEFECTS IN A CRYSTAL

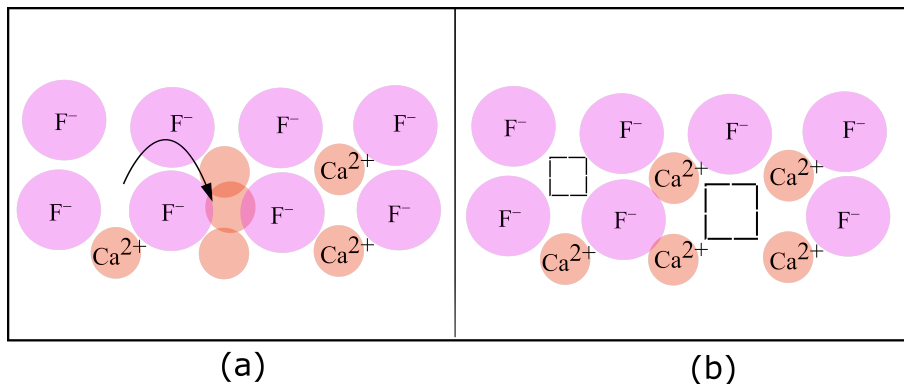


Fig. 1.2: (a) Schematic representation of a Frenkel defect in a crystal, created by the displacement of a positive ion. (b) Schematic of a Schottky defect, created by the displacement of a pair of positive and negative ions to the surface of the crystal.

Unfortunately, the nature of the electron traps, hole traps and recombination centers is known for very few materials. One well known example where the nature of the defects is known, are the *color centers* in natural crystals (Nassau [91]). Color centers can be, for example, a Frenkel defect in a crystal structure. These defects are generally introduced by extreme heat exciting and freeing electrons, or by irradiation. Color centers fall into two categories: *electron color centers* and *hole color centers*. In both cases, the color center is able to absorb only specific wavelengths, and the color one sees in these crystals is the complementary color of the absorbed wavelength.

Figure 1.3 shows an example of a color center in fluorite CaF_2 . Fluorite crystals consist of alternating calcium (Ca^{2+}) and fluorine ions (F^-). Every positive calcium ion is surrounded by negative fluorine ions, and vice versa. The electrical attraction between the positive and negative charges creates strong bonds in the crystal. Pure fluorite crystals are transparent, but natural fluorite exists in many colors, due to the presence of color centers.

One of these color centers is the purple *F center* or Frenkel defect of fluorite. Figure 1.3a is a two-dimensional representation of the CaF_2 structure. There are several ways by which an F^- ion can be missing from its usual position: this can occur during growth, or when energetic radiation displaces an F^- ion from its usual position to another point in the crystal. Such centers can also be created by growing fluorite in the presence of excess Ca, or by removing some F^- ions from the crystal by applying an electric field (Nassau [91]).

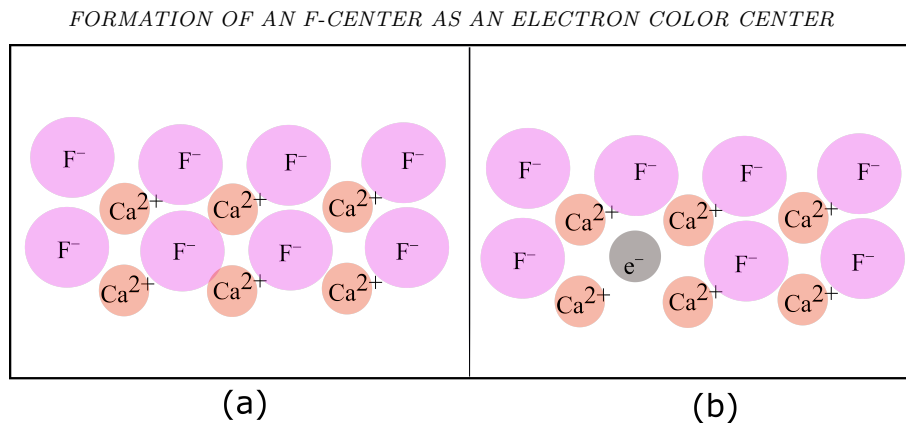


Fig. 1.3: Example of an electron color center. (a) 2D representation of a normal Fluorite CaF_2 crystal structure. (b) A fluorine ion has been displaced and the vacancy is replaced by an electron, forming an F-center or Frenkel defect in the form of an *electron color center*.

6 1 OVERVIEW OF LUMINESCENCE SIGNALS FROM DOSIMETRIC MATERIALS

Since the crystal must remain electrically neutral, an electron usually occupies the empty position to produce an *electron color center*, as shown in Fig.1.3b. This unpaired electron can now exist in excited states and new transitions are possible between energy states, leading to the coloration and fluorescence of these crystals.

For additional examples and a detailed presentation of the luminescence processes in quartz including vacancies, intrinsic defects and impurities, we refer to the detailed review article by Preusser et al. [130].

1.3 Thermoluminescence (TL) experiments and models

When the stimulation of the sample in the laboratory is thermal, the resulting signal is called *Thermoluminescence* (TL). Commonly used experimental heating functions during a TL experiment are linear, hyperbolic and exponential heating functions. During a TL experiment one records the light intensity as a function of temperature, and the total signal is termed a *TL glow curve*. An example of a TL glow curve measured for the dosimetric material BeO is shown in Fig.1.4a (Polymeris et al. [125]).

In this case the TL glow curve is simple and contains just one peak. The TL signal from this material could then be possibly described by a simple model, similar to the one shown in Fig.1.5. This is the simplest possible model which has been studied extensively in the literature, consisting of one trap and one recombination center (OTOR)). The application of the OTOR model for TL data is presented in detail in several chapters in this book.

The arrows in Fig.1.5 indicate electronic transitions, some of which involve transport of electrons and holes via the conduction and/or valence band. This type of model is termed a *delocalized transitions model*.

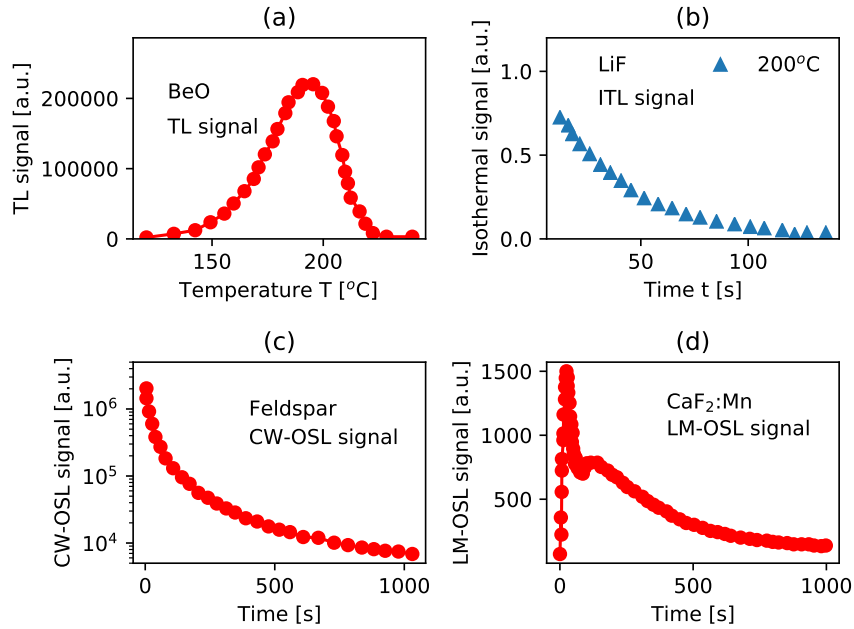


Fig. 1.4: Examples of luminescence signals from *delocalized transitions* (a) TL glow curve for the dosimetric material BeO (Polymeris et al. [125]); (b) ITL signal from LiF: Mg,Ti (Polymeris et al. [125]); (c) CW-OSL signal from feldspar sample KST4 (Pagonis et al. [115]); (d) LM-OSL signal from CaF₂:Mn (Kitis et al. [75])

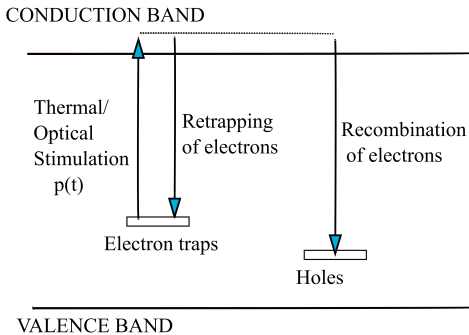


Fig. 1.5: Schematic representation of the *delocalized* transitions OTOR model, showing the various electronic transitions during thermal or optical excitation. Trapped electrons are raised into the conduction band, and are subsequently either retrapped in electron traps, or they recombine with holes at the recombination centers/hole traps

8.1 OVERVIEW OF LUMINESCENCE SIGNALS FROM DOSIMETRIC MATERIALS

The TL signals from a broad range of dosimetric materials can not be described by delocalized transitions models, and one must use instead a model similar to the one shown in Fig.1.6. By contrast to the OTOR model, the model shown in Fig.1.6 involves transitions between localized energy states, which do not involve the conduction or valence bands. This type of model is used to describe, for example, TL signals from feldspars, apatites and other dosimetric materials.

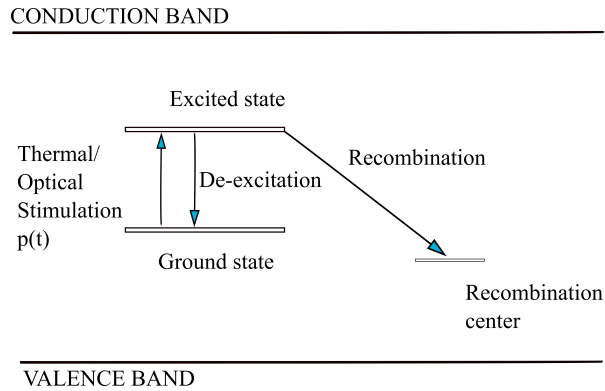


Fig. 1.6: Schematic representation of a *localized* transition model, in which electrons are raised from the ground state into an excited state, and are subsequently either de-excited into the ground state, or they can recombine with holes at the recombination centers/hole traps.

There are four major categories of delocalized models examined in detail in this book, namely the first order kinetics (FOK) model, general one trap model (GOT), mixed kinetics order model (MOK) and the empirical general order kinetics model (GOK). These models lead to analytical equations which are commonly used for the analysis of TL signals, and they are summarized in Fig.1.7, together with the relevant sections of this book. The last entry in Fig.1.7 is the excited state tunneling model (EST), which is a localized transitions model.

All differential equations in the TL models contain the Arrhenius thermal stimulation term $p(t)$ given by:

$$p(t) = s \exp \left[\frac{-E}{k_B T(t)} \right] \quad (1.1)$$

where E (eV) is the thermal activation energy of the trap, $k_B = 8.617 \times 10^{-5}$ eV/K is the Boltzmann factor, $T(t)$ (K) is the time dependent temperature of the sample, and s (s^{-1}) is the associated frequency factor. Typical values

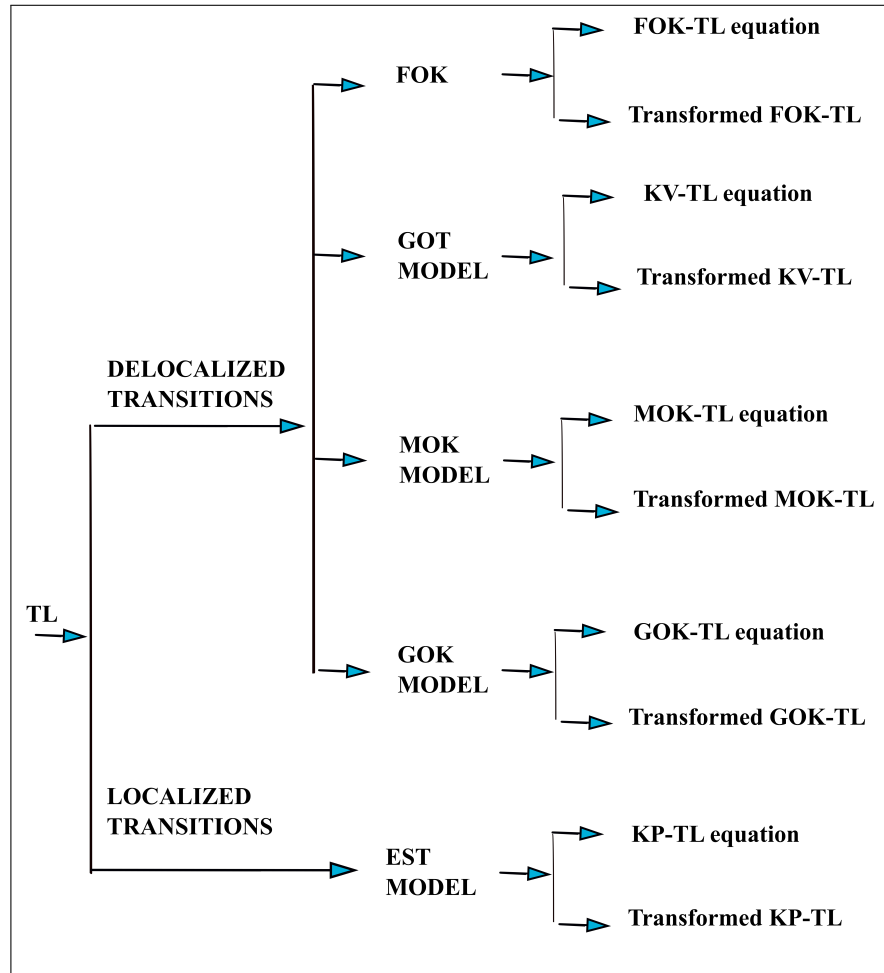


Fig. 1.7: Schematic diagram of the main models used for analyzing TL signals and the respective analytical equations. Four of these are *delocalized* transition models: the first order kinetics (FOK), general one trap (GOT), mixed order kinetics (MOK) and general order kinetics (GOK) empirical model. The excited state tunneling model (EST) is a *localized transitions* model.

of the frequency factor are $s = 10^8 - 10^{12} \text{ s}^{-1}$, and for the activation energy $E = 0.7 - 2 \text{ eV}$.

1.4 Isothermal luminescence (ITL) experiments and models

When the sample is stimulated at a constant temperature, the resulting signal is called *isothermal luminescence* (ITL). During an ITL experiment one records the light intensity as a function of elapsed time, and the total signal is termed a *ITL curve*. The excitation rate during an ITL experiment is:

$$p(t) = s \exp \left[\frac{-E}{k_B T_{ISO}} \right] \quad (1.2)$$

where T_{ISO} is the constant temperature during the ITL experiment. An example of an ITL curve measured for the dosimetric material BeO is shown in Fig.1.4b.

ITL signals can also be described by the FOK, GOT, MOK, GOK and EST models, similar to the situation for TL signals. These five models lead to analytical equations which are commonly used for the analysis of ITL signals, and they are summarized in Fig.1.8, together with the relevant sections of this book.

1.5 Optically stimulated luminescence (OSL) experiments and models

When the stimulation of a sample is optical using visible light, one is dealing with *optically stimulated luminescence* (OSL). Typically, blue LEDs with a wavelength of 470 nm are used during these OSL experiments. When the stimulation is with visible light and also occurs with a source of constant light intensity, the stimulated luminescence is termed *continuous wave optically stimulated luminescence* (CW-OSL), and the function $p(t)$ is given by:

$$p(t) = \sigma I \quad (1.3)$$

where $\sigma (\text{cm}^2)$ represents the optical cross section for the CW-OSL process, and $I (\text{photons cm}^{-2} \text{ s}^{-1})$ represents the photon flux. The units of the stimulation rate $p(t)$ are s^{-1} .

An example of a CW-OSL curve measured for a feldspar sample is shown in Fig.1.4c.

When the optical stimulation takes place using a source with an intensity which increases linearly with time, the stimulated luminescence is called

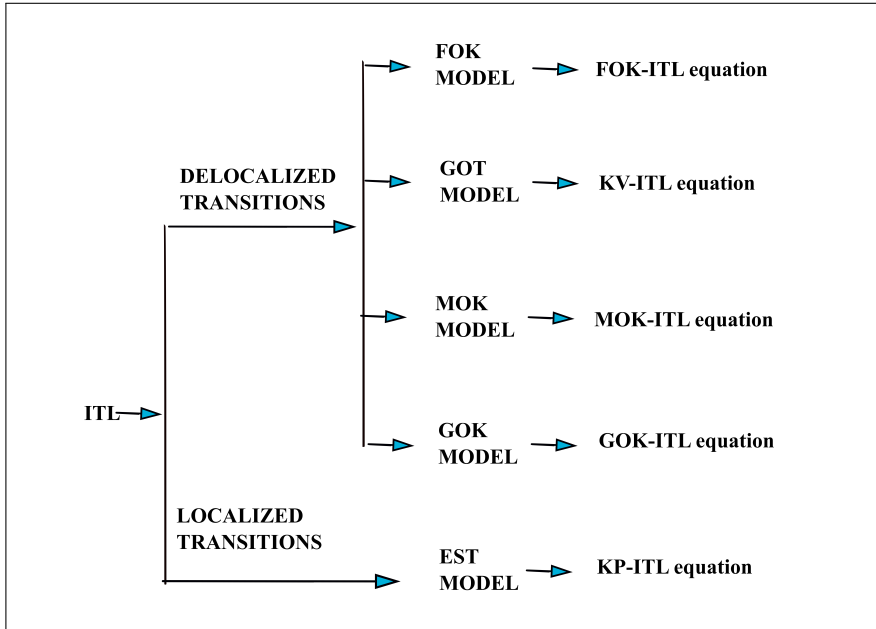


Fig. 1.8: Schematic diagram of the main delocalized and localized models which are used in this book for analysis of ITL signals, and the respective analytical equations. The *delocalized* transition models are: the first order kinetics (FOK), general one trap (GOT), mixed order kinetics (MOK) and general order kinetics (GOK) empirical model. The excited state tunneling model (EST) is a *localized transitions* model.

linearly modulated optically OSL (LM-OSL, and the stimulation rate $p(t)$ is given by:

$$p(t) = \frac{\sigma I}{P} t \quad (1.4)$$

where σ, I have the same meaning as in Eq.(1.3), t is the elapsed time and $P(s)$ is the total illumination time. An example of a LM-OSL curve measured for the dosimetric material $\text{CaF}_2:\text{Mn}$ is shown in Fig.1.4d.

During an LM-OSL experiment, the light intensity is recorded as a function of time, while increasing the stimulation linearly with time, thus obtaining a peak-shaped LM-OSL curve.

OSL signals can also be described by the FOK, GOT, MOK, GOK and EST models, similar to the situation for TL signals. These five models lead to analytical equations which are commonly used for the analysis of ITL signals, and they are summarized in Fig.1.9, together with the relevant sections of this book.

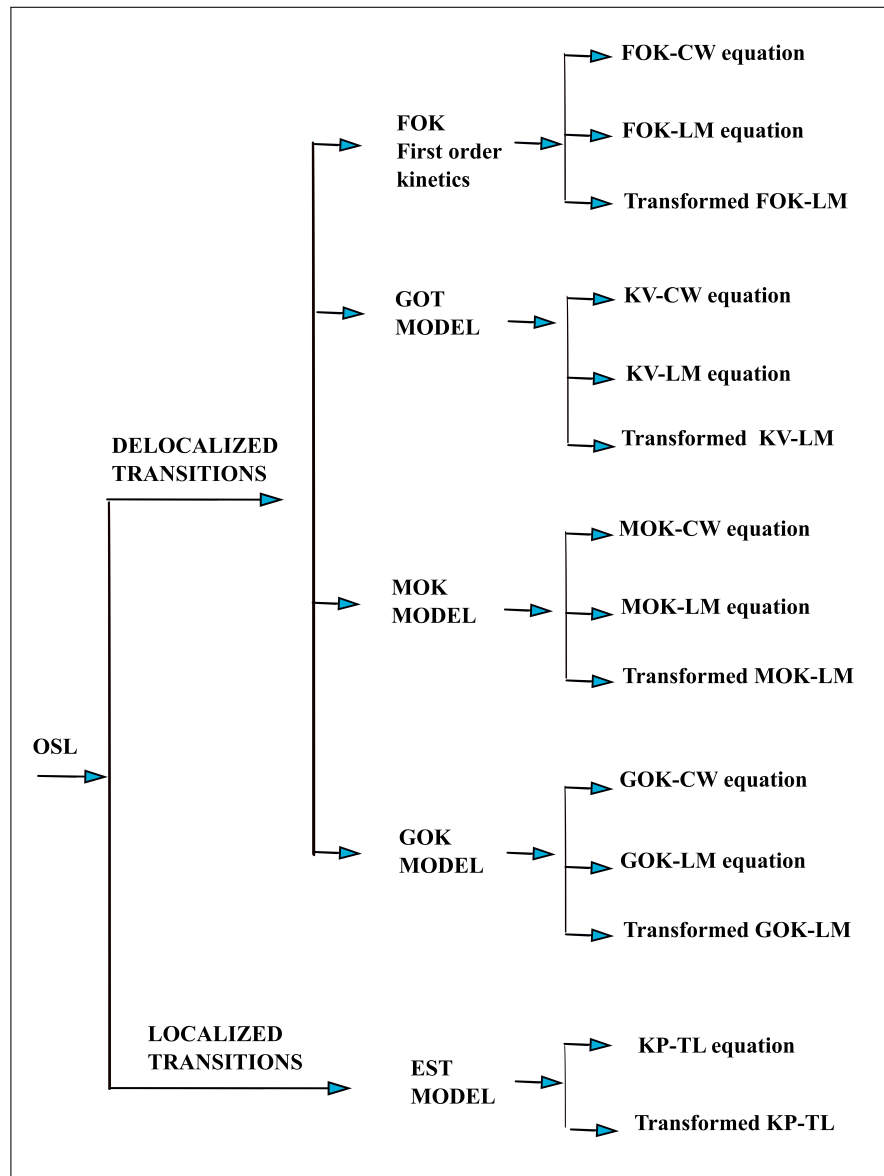


Fig. 1.9: The main *delocalized* models which are used for analysis of CW-OSL and LM-OSL signals, and the respective analytical equations. First order kinetics (FOK), general one trap (GOT), mixed order kinetics (MOK), empirical general order kinetics (GOK).

1.6 Infrared stimulated luminescence (IRSL) experiments and models

When the optical stimulation of the irradiated sample takes place with infrared photons, this process is called *infrared stimulated luminescence (IRSL)*. Typically infrared LEDs with a wavelength of 850 nm are used during these IRSL experiments. In this case $\sigma\text{ (cm}^2)$ in Eqs.(1.3) and (1.4) represents the corresponding *infrared* optical cross section for the IRSL process.

During CW-IRSL experiments the intensity of the light is kept constant, resulting in most cases in a monotonically decaying curve. Linear modulation of the infrared LEDs results in the production of a LM-IRSL signal

The shapes of CW-OSL and CW-IRSL signals are very similar to the shapes of CW-IRSL and LM-IRSL signals. However, these signals are obtained with very different wavelengths of light (470 nm for blue light LEDs and 850 nm for infrared LEDs). Extensive research has shown that the mechanisms involved in the production of these signals are very different. In the case of the CW-OSL and LM-OSL signals from most dosimetric materials, the mechanism is believed to involve the conduction band due to the higher energy of the blue LEDs, and can be described by a *delocalized* model similar to the OTOR model shown in Fig.1.5.

In the case of the CW-IRSL and LM-IRSL signals, the production mechanism is believed to involve localized energy levels located between the conduction and valence bands, as shown schematically previously in Fig.1.6. Two versions of this type of *localized transition model* have been used in the literature, the simple localized transition model (LT), and the tunneling localized transition model (TLT) which is based on quantum mechanical tunneling processes. Both of these types of models are implemented using Python in this book in subsequent chapters.

Figure 11.1 shows the EST model which leads to analytical equations commonly used for the analysis of CW-IRSL signals, together with the relevant sections of this book.

1.7 Time-resolved (TR) luminescence experiments and models

In a time-resolved (TR) experiment, optical stimulation is used to separate in time the stimulation and emission of luminescence. The luminescence is stimulated using a brief light pulse (usually from bright LEDs), and the emission is monitored during the stimulation (when the LED is ON), and also during the relaxation stages of the experiment (when the LEDs are OFF). The details of TR experimental setups can be found in the review article by Chithambo et al. [35].

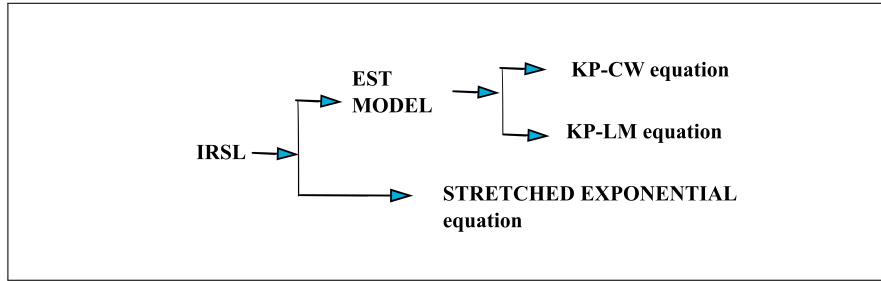


Fig. 1.10: Schematic diagram showing the *localized* model EST discussed in this book, and the respective analytical equations which are used for analysis of CW-IRSL and LM-IRSL signals.

TR techniques have been very useful in the study of luminescence mechanisms for a variety of dosimetric materials. The optical stimulation is carried out in a pulsed mode, giving rise to *pulsed OSL* and *pulsed IRSL* signals (POSL and PIRSL).

Figure 1.11 summarizes the models and analytical equations used in this chapter for analyzing TR signals. An example of TR-OSL experimental data from quartz is shown in Fig.1.12.

Figure 1.13 shows a different type of model used for describing TR signals, which contains both delocalized and localized electronic transitions.

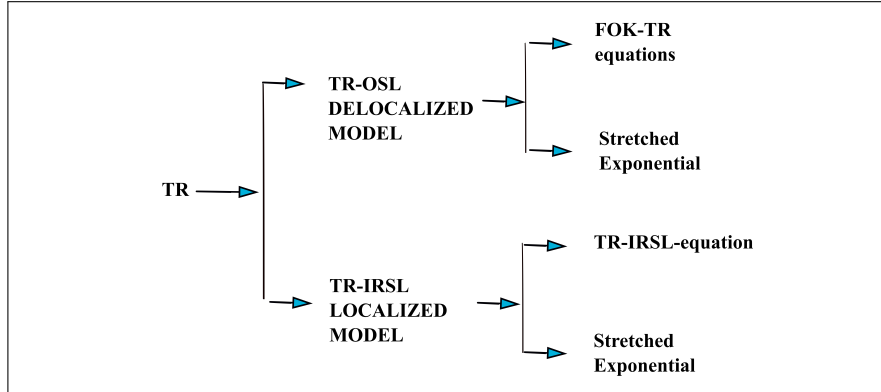


Fig. 1.11: Schematic diagram showing several models and the respective analytical equations which are used in this book for analysis of time-resolved luminescence signals.

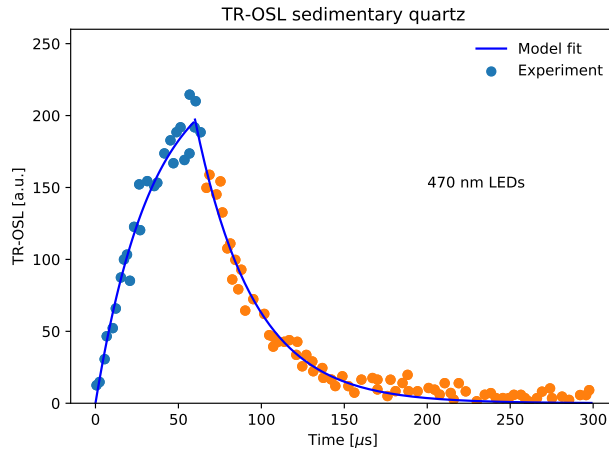


Fig. 1.12: Example of TR-OSL curves for sedimentary quartz with $60 \mu\text{s}$ pulse. For more details see Chithambo et al. [35].

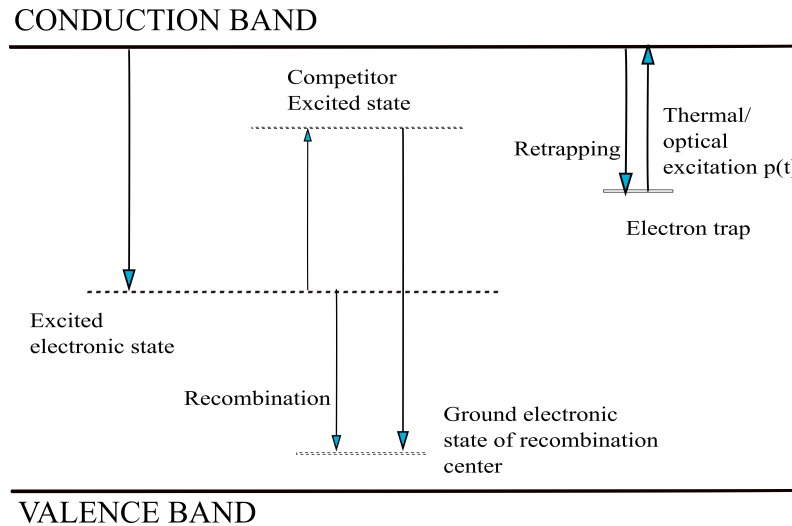


Fig. 1.13: A more complex luminescence model involving both delocalized and localized electronic transitions. Some of the transitions labeled are of a delocalized nature, while other transitions are internal transitions of a localized nature. For a detailed description of this thermal quenching model for quartz, see Pagonis et al. [97]

1.8 ESR and OA experiments: Correlations with luminescence signals

In this section we discuss briefly optical absorption (OA) and electron spin resonance (ESR) experiments, and point out their relationship to TL and OSL data. For a more complete review of these types of experiments in connection with TL/OSL data, the reader is referred to the ESR review paper by Trompier et al. [149], and also to the extended list of references in the book by Chen and Pagonis [31].

ESR and OA experiments are often measured simultaneously with TL and/or OSL in the same sample. These additional types of experiments produce important information about the underlying luminescence mechanisms, as well as about the nature of the trapping and luminescence centers.

The absorption technique is Electron spin (paramagnetic) resonance (ESR, EPR), is used for the study of materials which exhibit paramagnetism because of the magnetic moment of unpaired electrons. ESR spectra are usually presented as plots of the absorption or dispersion of the energy of an oscillating magnetic field of fixed radio frequency, versus the intensity of an applied static magnetic field. Among the wide variety of paramagnetic substances to which ESR spectroscopy has been applied, the one that is of interest in the present context is that of impurity centers in solids, mainly single crystals. Of course, the same impurity centers may be associated with TL, either acting as the charge-carrier traps, or as recombination centers. They may also be responsible for optical absorption. Since ESR is normally capable of identifying the impurities in the crystal, in cases where the simultaneous TL-ESR measurements show a direct relation between the two phenomena, the identification by ESR serves as a direct proof for the identity of the impurity involved in the TL process. Similarly to the OA case, it is normal that the ESR signal shows a decrease at a certain temperature range, where the trapping state becomes unstable. The instability may be associated with either the thermal release of charge carriers from the paramagnetic impurity, or, alternatively, the filling of paramagnetic impurities which serve as TL recombination centers. In both cases, it is expected that the TL peak will resemble the negative derivative of the ESR signal, with a close resemblance to OA.

The dose response of TL, OSL, OA and ESR signals exhibit nonlinear regions, associated with the phenomena of superlinearity and sublinearity. These are discussed in detail in a later chapter, in connection with recent theoretical research involving the Lambert W function.

Figure 1.14 shows simultaneous measurements and possible correlations between the TL, ESR and OA signals from a sample of fused silica [158]. This type of multiple facet experiment can be very useful in identifying the source of the various luminescence signals, i.e. the nature of the traps and centers in the dosimetric material.

1.9 What information can we extract from TL, ITL, OSL and TR luminescence signals?

Figure 1.16 is a schematic showing the two types of model used for describing the dose response of luminescence signals in this book. These are the OTOR model and the more complex two trap one recombination center (TTOR) model. These models and the respective analytical PKC and PKC-S equations are discussed in detail in the chapters on dose response of luminescence signals.

Figure 1.15 shows how the OTOR model can also be used to describe the electronic transitions during the irradiation of a dosimetric material.

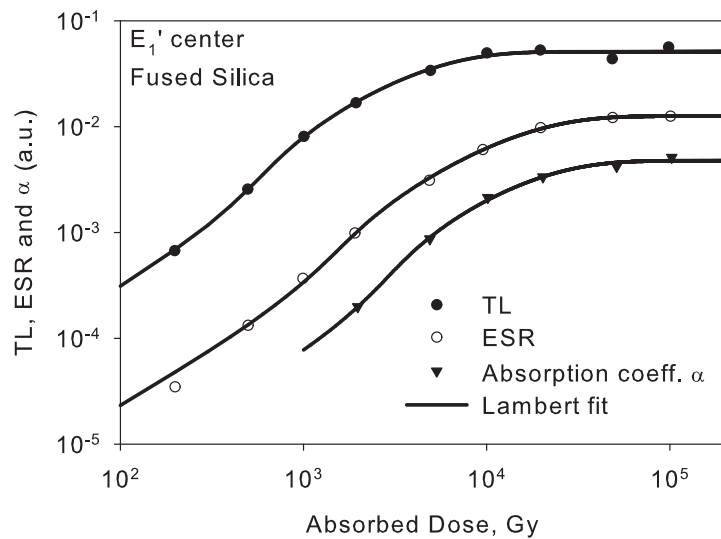


Fig. 1.14: Superlinear dose dependence of the E'_1 center concentration (ESR), TL and OA signals, from a single sample of fused silica. Note the log scale in both axes. For more details see Pagonis et al. [106], original data from Wieser [158].

1.9 What information can we extract from TL, ITL, OSL and TR luminescence signals?

The luminescence signals discussed in this chapter and in the rest of this book are obviously complex. The fundamental question for researchers is what kind of information they can extract from the experimental curves, and how.

In general, researchers would like to extract the following specific information:

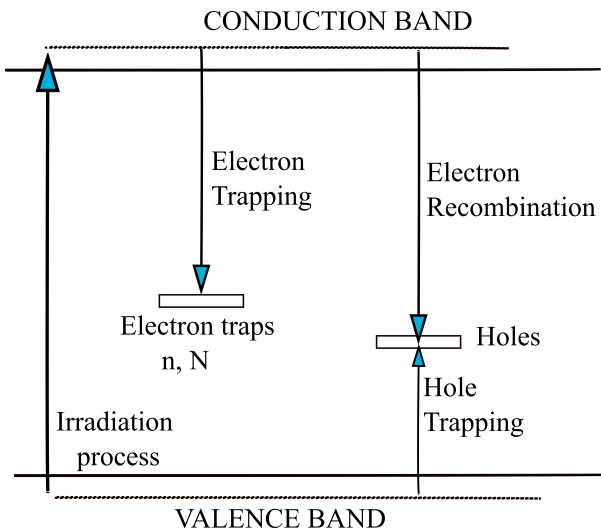


Fig. 1.15: The simplest OTOR model, showing the various electronic transitions during the irradiation stage. Irradiation creates electrons and holes in the conduction and valence bands, respectively. Electrons in the conduction band can subsequently either be trapped in electron traps, or they can recombine with holes at the recombination centers/hole traps. Holes in the valence band can be trapped in the same recombination centers/hole traps.

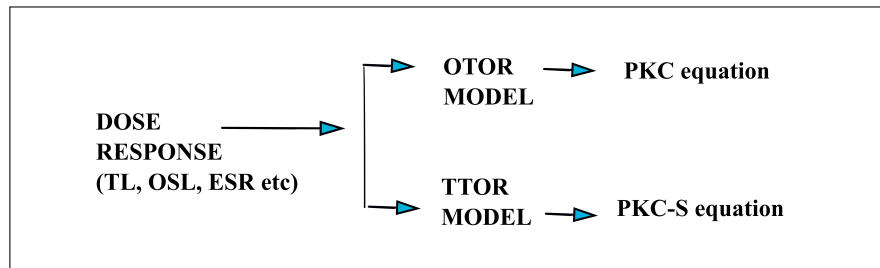


Fig. 1.16: Schematic diagram showing the two *delocalized* models OTOR and TTOR models discussed in this book, and the respective analytical equations which are used for analysis of the dose response of luminescence signals.

1.9 What information can we extract from TL, ITL, OSL and TR luminescence signals?

- The intensity of the light emitted during each stimulated luminescence effect, as a function of time or as a function of temperature.
- The *dose response*, i.e. the intensity of the light emitted as a function of irradiation dose.
- The basic physical parameters of the energy level responsible for the emission of light. For thermally stimulated processes these parameters are the activation energy E and the frequency factor s . For optically stimulated processes, they are the cross section σ for the corresponding process.
- Information on the physical mechanism behind the observed luminescence signals, and on the various processes involved.
- Information on whether the delocalized conduction and valence bands are involved in the luminescence processes, and whether localized energy transitions play a role in the production of the luminescence signals.

Luminescence signals from dosimetric materials are characterized by the presence of several components, originating from different traps or centers. These signals vary according to the preconditioning of the samples (irradiation dose, prior optical and thermal stimulation, radiation quality), and are described mathematically by phenomenological models based usually on systems of coupled differential equations.

As discussed in this chapter, two types of models that have been used extensively in the literature are *delocalized models* based on transitions involving the conduction and valence bands, and *localized models* usually involving different energy levels of the traps/centers. For a comprehensive historical summary of various types of luminescence models, the reader is referred for example to the book by Chen and Pagonis [31], and the review paper by McKeever and Chen [88]. The details of these models and their implementation with Python are given in several later chapters.

The main goals of *modeling* studies are:

- To provide a quantitative description of these dosimetric signals.
- To develop methods for the accurate evaluation of parameters characterizing traps and centers.
- To search for general models which explain the behavior of preconditioned samples.
- To help researchers understand the underlying luminescence production mechanisms.

References

1. G Adamiec, A Bluszcz, R Bailey, and M Garcia-Talavera. Finding model parameters: Genetic algorithms and the numerical modelling of quartz luminescence. *Radiation Measurements*, 41(7-8):897–902, 2006.
2. G Adamiec, M Garcia-Talavera, R M Bailey, and P I de La Torre. Application of a genetic algorithm to finding parameter values for numerical simulation of quartz luminescence. *Geochronometria*, 23:9–14, 2004.
3. D Afouxenidis, G S Polymeris, N C Tsirilganis, and G Kitis. Computerised curve deconvolution of TL/OSL curves using a popular spreadsheet program. *Radiation Protection Dosimetry*, 149:363–370, May 2012.
4. V Anechitei-Deacu, A Timar-Gabor, K J Thomsen, J-P Buylaert, M Jain, M Bailey, and A S Murray. Single and multi-grain OSL investigations in the high dose range using coarse quartz. *Radiation Measurements*, 120:124 – 130, 2018.
5. H G Balian and N W Eddy. Figure-of-merit (FOM), an improved criterion over the normalized chi-squared test for assessing goodness-of-fit of gamma-ray spectral peaks. *Nuclear Instruments and Methods*, 145:389–395, 1977.
6. R. Battiti and G. Tecchiolli. Simulated annealing and Tabu search in the long run: A comparison on QAP tasks. *Computers & Mathematics with Applications*, 28(6):1 – 8, 1994.
7. G W Berger. Regression and error analysis for a saturating-exponential-plus-linear model. *Ancient TL*, 8(3):23–25, 1990.
8. G W Berger and R Chen. Error analysis and modelling of double saturating exponential dose response curves from SAR OSL dating. *Ancient TL*, 29(1):9–14, 2011.
9. R H Biswas, F Herman, G E King, and J Braun. Thermoluminescence of feldspar as a multi-thermochronometer to constrain the temporal variation of rock exhumation in the recent past. *Earth and Planetary Science Letters*, 495:56–68, 2018.
10. R H Biswas, F Herman, G E King, B Lehmann, and A K Singhvi. Surface paleothermometry using low-temperature thermoluminescence of feldspar. *Climate of the Past*, 16(6):2075–2093, 2020.
11. L Bøtter-Jensen, S W S McKeever, and A G Wintle. *Optically Stimulated Luminescence Dosimetry*. Elsevier Science, 2003.
12. A J J Bos. Thermoluminescence as a research tool to investigate luminescence mechanisms. *Materials (Basel, Switzerland)*, 10, November 2017.
13. A J J Bos, T M Piters, J M Gómez-Ros, and A Delgado. An Intercomparison of Glow Curve Analysis Computer Programs: I. Synthetic Glow Curves. *Radiation protection dosimetry*, 47:473–477, 1993.
14. A.J.J. Bos, T.M. Piters, J.M. Gómez Ros, and A. Delgado. An Intercomparison of Glow Curve Analysis Computer Programs: II. Measured Glow Curves. *Radiation Protection Dosimetry*, 51(4):257–264, 02 1994.

15. J J Bosken and C Schmidt. Direct and indirect luminescence dating of tephra: A review. *Journal of Quaternary Science*, 35(1-2):39–53, 2020.
16. S G E Bowman and R Chen. Superlinear filling of traps in crystals due to competition during irradiation. *Journal of Luminescence*, 18-19:345 – 348, 1979.
17. N D Brown, E J Rhodes, and T M Harrison. Using thermoluminescence signals from feldspars for low-temperature thermochronology. *Quat. Geochronol.*, 42:31–41, 2017.
18. N.D. Brown and E.J. Rhodes. Dose-rate dependence of natural TL signals from feldspars extracted from bedrock samples. *Radiation Measurements*, 128:106188, 2019.
19. E Bulur. An alternative technique for optically stimulated luminescence (OSL) experiment. *Radiation Measurements*, 26(5):701–709, 1996.
20. E Bulur. A simple transformation for converting CW-OSL curves to LM-OSL curves. *Radiation Measurements*, 32(2):141–145, 2000.
21. E Bulur and H Y Göksu. Infrared (IR) stimulated luminescence from feldspars with linearly increasing excitation light intensity. *Radiation Measurements*, 30:505–512, 1999.
22. E Bulur and A Yeltik. Optically stimulated luminescence from BeO ceramics: An LM-OSL study. *Radiation Measurements*, 45:29–34, 2010.
23. I F Chang and P Thioulouse. Treatment of thermostimulated luminescence, phosphorescence, and photostimulated luminescence with a tunneling theory. *Journal of Applied Physics*, 53(8):5873–5875, 1982.
24. R Chen. Glow curves with general order kinetics. *Journal of The Electrochemical Society*, 116:1254, 1969.
25. R Chen. On the calculation of activation energies and frequency factors from glow curves. *Journal of Applied Physics*, 40:570–585, 1969.
26. R. Chen. Apparent stretched-exponential luminescence decay in crystalline solids. *Journal of Luminescence*, 102-103:510–518, May 2003.
27. R. Chen and N. Kristianpoller. Investigation of Phosphorescence Decay Using TL-like Presentation. *Radiation Protection Dosimetry*, 17(1-4):443–446, 12 1986.
28. R Chen, N Kristianpoller, Z Davidson, and R Visocekas. Mixed first and second order kinetics in thermally stimulated processes. *Journal of Luminescence*, 23:293–303, 1981.
29. R Chen and S W S McKeever. Characterization of nonlinearities in the dose dependence of thermoluminescence. *Radiation Measurements*, 23(4):667 – 673, 1994.
30. R Chen and S W S McKeever. *Theory of thermoluminescence and related phenomena*. World Scientific, Singapore, 1997.
31. R Chen and V Pagonis. *Thermally and Optically Stimulated Luminescence: A Simulation Approach*. John Wiley & Sons, Chichester, 2011.
32. Reuven Chen and PL Leung. The decay of OSL signals as stretched-exponential functions. *Radiation measurements*, 37(4):519–526, 2003.
33. M L Chithambo. The analysis of time-resolved optically stimulated luminescence: I. theoretical considerations. *Journal of Physics D: Applied Physics*, 40(7):1874, 2007.
34. M L Chithambo. The analysis of time-resolved optically stimulated luminescence: II. computer simulations and experimental results. *Journal of Physics D: Applied Physics*, 40(7):1880, 2007.
35. M L Chithambo, C Ankjærgaard, and V Pagonis. Time-resolved luminescence from quartz: An overview of contemporary developments and applications. *Physica B: Condensed Matter*, 481:8–18, 2016.
36. M L Chithambo and R B Galloway. A pulsed light-emitting-diode system for stimulation of luminescence. *Measurement Science and Technology*, 11(4):418–424, mar 2000.
37. Makaiko L. Chithambo. *An Introduction to Time-Resolved Optically Stimulated Luminescence*. 2053-2571. Morgan and Claypool Publishers, 2018.

38. K.S. Chung, H.S. Choe, J.I. Lee, and J.L. Kim. An algorithm for the deconvolution of the optically stimulated luminescence glow curves involving the mutual interactions among the electron traps. *Radiation Measurements*, 46(12):1598 – 1601, 2011.
39. K.S. Chung, J.I. Lee, and J.L. Kim. A computer program for the deconvolution of the thermoluminescence glow curves by employing the interactive trap model. *Radiation Measurements*, 47(9):766 – 769, 2012.
40. K.S. Chung, C.Y. Park, J.I. Lee, and J.L. Kim. Thermoluminescence glow curve deconvolution of LiF:Mg,Cu,Si with more realistic kinetic models. *Radiation Measurements*, 59:151 – 154, 2013.
41. R J Clark and I K Bailiff. Fast time-resolved luminescence emission spectroscopy in some feldspars. *Radiation Measurements*, 29(5):553 – 560, 1998.
42. R M Corless, G H Gonnet, D G E Hare, D J Jerey, and D E Knuth. On the Lambert W function. *Advances in Computational Mathematics*, 5:329–359, 1996.
43. R M Corless, D J Jerey, and D E Knuth. A sequence series for the Lambert W function. In *Proceedings of the International Symposium on Symbolic and Algebraic Computation , ISSAC*, pages 133–140, 1997.
44. Olivier Q. De Clercq, Jiaren Du, Philippe F. Smet, Jonas J. Joos, and Dirk Poelman. Predicting the afterglow duration in persistent phosphors: a validated approach to derive trap depth distributions. *Phys. Chem. Chem. Phys.*, 20:30455–30465, 2018.
45. M Duval. Dose response curve of the ESR signal of the aluminum center in quartz grains extracted from sediment. *Ancient TL*, 30(2):1–9, 2012.
46. J M Edmund. *Effects of temperature and ionization density in medical luminescence dosimetry using Al₂O₃:C (PhD Thesis, Riso, Denmark)*. PhD thesis, Risø National Laboratory, 2007. Risø-PhD-38(EN).
47. M Fuchs, S Kreutzer, D Rousseau, P Antoine, C Hatté, F Lagroix, O Moine, C Gauthier, J Svoboda, and L Lisá. The loess sequence of Dolní Věstonice, Czech Republic: A new OSL-based chronology of the last climatic cycle. *Boreas*, 42(3):664–677, 2013.
48. G F J Garlick and A F Gibson. The electron trap mechanism of luminescence in sulphide and silicate phosphors. *Proceedings of the Physical Society*, 60:574–590, 1948.
49. J M Gómez-Ros and G Kitit. Computerized glow-curve deconvolution using mixed and general order kinetics. *Radiation Protection Dosimetry*, 101:47–52, 2002.
50. B Guralnik, B Li, M Jain, R Chen, R B Paris, A S Murray, S Li, V Pagonis, P G Valla, and F Herman. Radiation-induced growth and isothermal decay of infrared-stimulated luminescence from feldspar. *Radiation Measurements*, 81:224 – 231, 2015.
51. A Halperin and A A Brainer. Evaluation of thermal activation energies from glow curves. *Physical Review*, 117:408–415, 1960.
52. A Halperin and R Chen. Thermoluminescence of semiconducting diamonds. *Phys. Rev.*, 148:839–845, Aug 1966.
53. Y Horowitz, E Fuks, H Datz, L Oster, J Livingstone, and A Rosenfeld. Mysteries of LiF TLD response following high ionization density irradiation: Glow curve shapes, dose response, the unified interaction model and modified track structure theory. *Radiation Measurements*, 46(12):1342 – 1348, 2011.
54. Y S Horowitz. The theoretical and microdosimetric basis of thermoluminescence and applications to dosimetry. *Physics in medicine and biology*, 26:765–824, Sep 1981.
55. Y.S. Horowitz and D. Yossian. Computerised Glow Curve Deconvolution: Application to Thermoluminescence Dosimetry. *Radiation Protection Dosimetry*, 60(1):3–3, 06 1995.
56. D J Huntley. An explanation of the power-law decay of luminescence. *Journal of Physics: Condensed Matter*, 18(4):1359, 2006.
57. D J Huntley and M Lamothe. Ubiquity of anomalous fading in K-feldspars and the measurement and correction for it in optical dating. *Canadian Journal of Earth Sciences*, 38(7):1093–1106, 2001.

58. D J Huntley and Olav B Lian. Some observations on tunnelling of trapped electrons in feldspars and their implications for optical dating. *Quaternary Science Reviews*, 25(19-20):2503–2512, 2006.
59. M Jain, B Guralnik, and M T Andersen. Stimulated luminescence emission from localized recombination in randomly distributed defects. *Journal of Physics: Condensed Matter*, 24(38):385402, 2012.
60. M. Jain, A.S. Murray, and L. BÄttter-Jensen. Characterisation of blue-light stimulated luminescence components in different quartz samples: implications for dose measurement. *Radiation Measurements*, 37(4):441–449, 2003. Proceedings of the 10th international Conference on Luminescence and Electron-Spin Resonance Dating (LED 2002).
61. M Jain, R Sohbati, B Guralnik, A S Murray, M Kook, T Lapp, A K Prasad, K J Thomson, and J P Buylaert. Kinetics of infrared stimulated luminescence from feldspars. *Radiation Measurements*, 81:242 – 250, 2015.
62. R H Kars and J Wallinga. IRSL dating of K-feldspars: Modelling natural dose response curves to deal with anomalous fading and trap competition. *Radiation Measurements*, 44(5):594–599, 2009.
63. R Katz. Track structure theory in radiobiology and in radiation detection. *Nuclear Track Detection*, 2(1):1 – 28, 1978.
64. G E King, B Guralnik, P G Valla, and F Herman. Trapped-charge thermochronometry and thermometry: A status review. *Chemical Geology*, 44:3–17, 2016.
65. G E King, F Herman, R Lambert, P G Valla, and B Guralnik. Multi OSL thermochronometry of feldspar. *Quaternary Geochronology*, 33:76–87, 2016.
66. G. Kitis. Confirmation of the influence of thermal quenching on the initial rise method in alpha Al₂O₃:C. *physica status solidi (a)*, 191(2):621–627, 2002.
67. G. Kitis, E. Carinou, and P. Askounis. Glow-curve de-convolution analysis of TL glow-curve from constant temperature hot gas TLD readers. *Radiation Measurements*, 47:258 – 265, 2012.
68. G Kitis, C Furetta, and V Pagonis. Mixed-order kinetics model for optically stimulated luminescence. *Modern Physics Letters B*, 23(27):3191–3207, 2009.
69. G Kitis and J M Gómez-Ros. Glow curve deconvolution functions for mixed order kinetics and a continuous trap distribution. *Nucl. Instrum. Methods A* 440, 440:224–231, 1999.
70. G Kitis, J M Gómez-Ros, and J W N Tuyn. Thermoluminescence glow curve deconvolution functions for first, second and general order kinetics. *J. Phys. D: Appl. Phys.*, 31:2666–2646, 1998.
71. G Kitis, N Kiyak, G S Polymeris, and N C Tsirliganis. The correlation of fast OSL component with the TL peak at in quartz of various origins. *Journal of Luminescence*, 130:298–303, 2010.
72. G Kitis and V Pagonis. Computerized curve deconvolution analysis for LM-OSL. *Radiation Measurements*, 43:737 – 741, 2008.
73. G Kitis and V Pagonis. Analytical solutions for stimulated luminescence emission from tunneling recombination in random distributions of defects. *Journal of Luminescence*, 137:109–115, 2013.
74. G Kitis and V Pagonis. Properties of thermoluminescence glow curves from tunneling recombination processes in random distributions of defects. *Journal of Luminescence*, 153:118–124, 2014.
75. G Kitis, G S Polymeris, and V Pagonis. Stimulated luminescence emission: From phenomenological models to master analytical equations. *Applied Radiation and Isotopes*, 153:108797, 2019.
76. G Kitis, G S Polymeris, E Sahiner, N Meric, and V Pagonis. Influence of the infrared stimulation on the optically stimulated luminescence in four K-feldspar samples. *Journal of Luminescence*, 176:32 – 39, 2016.

77. G Kitis, G S Polymeris, I K Sfampa, M Prokic, N Meriç, and V Pagonis. Prompt isothermal decay of thermoluminescence in Mg_4BO_7 : Dy, Na and Li_4BO_7 :Cu,In dosimeters. *Radiation Measurements*, 84:15–25, 2016.
78. G. Kitis, G.S. Polymeris, V. Pagonis, and N.C. Tsirliganis. Anomalous fading of OSL signals originating from very deep traps in durango apatite. *Radiation Measurements*, 49:73 – 81, 2013.
79. G Kitis and N D Vlachos. General semi-analytical expressions for TL, OSL and other luminescence stimulation modes derived from the OTOR model using the Lambert W-function. *Radiation Measurements*, 48:47 – 54, 2013.
80. M Lamothe, M Auclair, C Hamzaoui, and S Huot. Towards a prediction of long-term anomalous fading of feldspar IRSL. *Radiation Measurements*, 37(4):493–498, 2003.
81. J L Lawless, R Chen, and V Pagonis. Sublinear dose dependence of thermoluminescence and optically stimulated luminescence prior to the approach to saturation level. *Radiation Measurements*, 44(5):606–610, 2009.
82. P W Levy. Overview Of Nuclear Radiation Damage Processes: Phenomenological Features Of Radiation Damage In Crystals And Glasses. In Paul W. Levy, editor, *Radiation Effects on Optical Materials*, volume 0541, pages 2 – 24. International Society for Optics and Photonics, SPIE, 1985.
83. B Li, Z Jacobs, and R G Roberts. Investigation of the applicability of standardised growth curves for OSL dating of quartz from Haia Fteah cave, Libya. *Quaternary Geochronology*, 35:1 – 15, 2016.
84. B Li and S H Li. Investigations of the dose-dependent anomalous fading rate of feldspar from sediments. *Journal of Physics D: Applied Physics*, 41(22):225502, 2008.
85. S E Lowick, F Preusser, and A G Wintle. Investigating quartz optically stimulated luminescence dose response curves at high doses. *Radiation Measurements*, 45(9):975 – 984, 2010.
86. C E May and J A Partridge. Thermoluminescent kinetics of alpha-irradiated alkali halides. *The Journal of Chemical Physics*, 40(5):1401–1409, 1964.
87. S W S McKeever. Thermoluminescence of solids. Cambridge University Press, 1985.
88. S W S McKeever and R Chen. Luminescence models. *Radiation Measurements*, 27(5):625–661, 1997.
89. E F Mischa and S W S McKeever. Mechanisms of Supralinearity in Lithium Fluoride Thermoluminescence Dosimeters. *Radiation Protection Dosimetry*, 29(3):159–175, 11 1989.
90. P Morthekai, J Thomas, M S Pandian, V Balaran, and A K Singhvi. Variable range hopping mechanism in band-tail states of feldspars: A time-resolved irsl study. *Radiation Measurements*, 47(9):857 – 863, 2012.
91. K Nassau. The physics and chemistry of color: the fifteen causes of color, the physics and chemistry of color: The fifteen causes of color, by kurt nassau. Technical report, ISBN 0-471-39106-9. Wiley-VCH, 2001.
92. S V Nikiforov, V S Kortov, and M G Kazantseva. Simulation of the superlinearity of dose characteristics of thermoluminescence of anion-defective aluminum oxide. *Physics of the Solid State*, 56(3):554–560, March 2014.
93. S V Nikiforov, I I Milman, and V S Kortov. Thermal and optical ionization of F-centers in the luminescence mechanism of anion-defective corundum crystals. *Radiation Measurements*, 33(5):547 – 551, 2001. Proceedings of the International Symposium on Luminescent Detectors and Transformers of Ionizing Radiation.
94. V. Pagonis. *Luminescence: Data Analysis and Modeling Using R*. Use R! Springer International Publishing, 2021.
95. V Pagonis, C Ankjærgaard, M Jain, and R Chen. Thermal dependence of time-resolved blue light stimulated luminescence in $Al_2O_3:C$. *Journal of Luminescence*, 136:270–277, 2013.
96. V Pagonis, C Ankjærgaard, M Jain, and M L Chithambo. Quantitative analysis of time-resolved infrared stimulated luminescence in feldspars. *Physica B: Condensed Matter*, 497:78–85, 2016.

97. V Pagonis, C Ankjærgaard, A S Murray, M Jain, R Chen, J Lawless, and S Greilich. Modelling the thermal quenching mechanism in quartz based on time-resolved optically stimulated luminescence. *Journal of Luminescence*, 130(5):902–909, 2010.
98. V Pagonis, N Brown, G S Polymeris, and G Kitis. Comprehensive analysis of thermoluminescence signals in Mg_4BO_7 : Dy, Na dosimeter. *Journal of Luminescence*, 213:334 – 342, 2019.
99. V Pagonis, R Chen, C Kulp, and G Kitis. An overview of recent developments in luminescence models with a focus on localized transitions. *Radiation Measurements*, 106:3 – 12, 2017.
100. V Pagonis, R Chen, Maddrey J W, and Sapp B. Simulations of time-resolved photoluminescence experiments in $Al_2O_3:C$. *Journal of Luminescence*, 131(5):1086–1094, 2011.
101. V Pagonis, J Friedrich, M Discher, A Müller-Kirschbaum, V Schlosser, S Kreutzer, R Chen, and C Schmidt. Excited state luminescence signals from a random distribution of defects: A new Monte Carlo simulation approach for feldspar. *Journal of Luminescence*, 207:266–272, 2019.
102. V Pagonis, M Jain, K J Thomsen, and A S Murray. On the shape of continuous wave infrared stimulated luminescence signals from feldspars: A case study. *Journal of Luminescence*, 153:96–103, 2014.
103. V Pagonis and G Kitis. Prevalence of first-order kinetics in thermoluminescence materials: An explanation based on multiple competition processes. *Physica Status Solidi B*, 249:1590–1601, 2012.
104. V Pagonis and G Kitis. Mathematical aspects of ground state tunneling models in luminescence materials. *Journal of Luminescence*, 168:137–144, 2015.
105. V Pagonis, G Kitis, and R Chen. A new analytical equation for the dose response of dosimetric materials, based on the Lambert W function. *Journal of Luminescence*, 225:117333, 2020.
106. V Pagonis, G Kitis, and R Chen. Superlinearity revisited: A new analytical equation for the dose response of defects in solids, using the Lambert W function. *Journal of Luminescence*, 227:117553, 2020.
107. V Pagonis, G Kitis, and C Furetta. *Numerical and practical exercises in thermoluminescence*. Springer Science & Business Media, 2006.
108. V Pagonis and C Kulp. Monte Carlo simulations of tunneling phenomena and nearest neighbor hopping mechanism in feldspars. *Journal of Luminescence*, 181:114–120, 2017.
109. V Pagonis, C Kulp, C Chaney, and M Tachiya. Quantum tunneling recombination in a system of randomly distributed trapped electrons and positive ions. *Journal of Physics. Condensed matter*, 29:365701, 2017.
110. V Pagonis, J L Lawless, R Chen, and ML Chithambo. Analytical expressions for time-resolved optically stimulated luminescence experiments in quartz. *Journal of Luminescence*, 131(9):1827–1835, 2011.
111. V Pagonis, S M Mian, M L Chithambo, E Christensen, and C Barnold. Experimental and modelling study of pulsed optically stimulated luminescence in quartz, marble and beta irradiated salt. *Journal of Physics D: Applied Physics*, 42(5):055407, 2009.
112. V Pagonis, S M Mian, and G Kitis. Fit of first order thermoluminescence glow peaks using the weibull distribution function. *Radiation protection dosimetry*, 93:11–17, 2001.
113. V Pagonis, P Morthekai, A K Singhvi, J Thomas, V Balaram, G Kitis, and R Chen. Time-resolved infrared stimulated luminescence signals in feldspars: Analysis based on exponential and stretched exponential functions. *Journal of Luminescence*, 132(9):2330–2340, 2012.
114. V Pagonis, H Phan, D Ruth, and G Kitis. Further investigations of tunneling recombination processes in random distributions of defects. *Radiation Measurements*, 58:66 – 74, 2013.

115. V Pagonis, G S Polymeris, and G Kitis. On the effect of optical and isothermal treatments on luminescence signals from feldspars. *Radiation Measurements*, 82:93–101, 2015.
116. Vasilis Pagonis, Nathan D. Brown, Jun Peng, George Kitis, and George S. Polymeris. On the deconvolution of promptly measured luminescence signals in feldspars. *Journal of Luminescence*, 239:118334, 2021.
117. Vasilis Pagonis, George Kitis, and George S. Polymeris. Quantum tunneling processes in feldspars: Using thermoluminescence signals in thermochronometry. *Radiation Measurements*, 134:106325, 2020.
118. Vasilis Pagonis, Christoph Schmidt, and Sebastian Kreutzer. Simulating feldspar luminescence phenomena using R. *Journal of Luminescence*, 235:117999, 2021.
119. J Peng, Z Dong, and F Han. tgcd: An R package for analyzing thermoluminescence glow curves. *SoftwareX*, 5:112–120, 2016.
120. S A Petrov and I K Bailiff. Thermal quenching and the initial rise technique of trap depth evaluation. *Journal of Luminescence*, 65(6):289–291, 1996.
121. S A Petrov and I K Bailiff. Determination of trap depths associated with tl peaks in synthetic quartz (350–550 k). *Radiation Measurements*, 27(2):185–191, 1997.
122. E. B. Podgorsak, P. R. Moran, and J. R. Cameron. Interpretation of resolved glow curve shapes in LiF(TLD-100) from 100 to 500K. pp 1-8 of *Proceedings of the Third International Conference on Luminescence Dosimetry*. /Mejdahl, V. (ed.). Risoe, Denmark Danish Atomic Energy Commission (1971), 1971.
123. G S Polymeris. OSL at elevated temperatures: Towards the simultaneous thermal and optical stimulation. *Radiation Physics and Chemistry*, 106:184 – 192, 2015.
124. G S Polymeris, V Pagonis, and G Kitis. Thermoluminescence glow curves in preheated feldspar samples: An interpretation based on random defect distributions. *Radiation Measurements*, 97:20 – 27, 2017.
125. G S Polymeris, V Pagonis, and G Kitis. Investigation of thermoluminescence processes during linear and isothermal heating of dosimetric materials. *Journal of Luminescence*, 222:117142, 2020.
126. G S Polymeris, N Tsirliganis, Z Loukou, and G Kitis. A comparative study of the anomalous fading effects of TL and OSL signals of Durango apatite. *Physica Status Solidi (a)*, 203(3):578–590, 2006.
127. GS Polymeris, E Theodosoglou, G Kitis, NC Tsirliganis, A Koroneos, and KM Paraskevopoulos. Preliminary results on structural state characterization of K-feldspars by using thermoluminescence. *Mediterranean Archaeology and Archaeometry*, 13(3):155–161, 2013.
128. N R J Poolton, K B Ozanyan, J Wallinga, A S Murray, and L Bøtter-Jensen. Electrons in feldspar II: a consideration of the influence of conduction band-tail states on luminescence processes. *Physics and Chemistry of Minerals*, 29(3):217–225, 2002.
129. N R J Poolton, J Wallinga, A S Murray, E Bulur, and L Bøtter-Jensen. Electrons in feldspar I: on the wavefunction of electrons trapped at simple lattice defects. *Physics and Chemistry of Minerals*, 29(3):210–216, April 2002.
130. F Preusser, M Chithambo, T Götte, M Martini, K Ramseyer, E J Sendezera, G Susino, and A G Wintle. Quartz as a natural luminescence dosimeter. *Earth-Science Reviews*, 97(1):184–214, 2009.
131. M. Puchalska and P. Bilski. Glowfit-a new tool for thermoluminescence glow-curve deconvolution. *Radiation Measurements*, 41(6):659 – 664, 2006.
132. J T Randall and M H F Wilkins. Phosphorescence and electron traps. I. The study of trap distributions. *Proceedings of the Royal Society of London A: Mathematical, Physical and Engineering Sciences*, 184(999):366–389, 1945.
133. M S Rasheedy. On the general-order kinetics of the thermoluminescence glow peak. *J. Phys.: Condens. Matter*, 5:633–636, 1993.
134. A M Sadek, H M Eissa, A M Basha, E Carinou, P Askounis, and G Kitis. The deconvolution of thermoluminescence glow-curves using general expressions derived from

- the one trap-one recombination (OTOR) level model. *Applied radiation and isotopes : including data, instrumentation and methods for use in agriculture, industry and medicine*, 95:214–221, January 2015.
135. E Şahiner, G Kitis, V Pagonis, N Meriç, and G S Polymeris. Tunnelling recombination in conventional, post-infrared and post-infrared multi-elevated temperature IRSL signals in microcline K-feldspar. *Journal of Luminescence*, 188:514–523, 2017.
 136. D C W Sanderson and R J Clark. Pulsed photostimulated luminescence of alkali feldspars. *Radiation Measurements*, 23(2):633 – 639, 1994.
 137. I K Sfampa, G S Polymeris, V Pagonis, E Theodosoglou, N.C. Tsirliganis, and G. Kitis. Correlation of basic TL, OSL and IRSL properties of ten K-feldspar samples of various origins. *Nuclear Instruments and Methods in Physics Research Section B: Beam Interactions with Materials and Atoms*, 359:89 – 98, 2015.
 138. I K Sfampa, G S Polymeris, N Tsirliganis, V Pagonis, and G Kitis. Prompt isothermal decay of thermoluminescence in an apatite exhibiting strong anomalous fading. *Nuclear Instruments and Methods in Physics Research Section B: Beam Interactions with Materials and Atoms*, 320:57–63, 2014.
 139. Ioanna K. Sfampa, George S. Polymeris, Vasilis Pagonis, and George Kitis. Correlation between isothermal TL and IRSL in K-Feldspars of various types. *Radiation Physics and Chemistry*, 165:108386, 2019.
 140. J S Singarayer and R M Bailey. Further investigations of the quartz optically stimulated luminescence components using linear modulation. *Radiation Measurements*, 37(4):451–458, 2003.
 141. L L Singh and R K Gartia. Theoretical derivation of a simplified form of the OTOR/GOT differential equation. *Radiation Measurements*, 59:160 – 164, 2013.
 142. Bhagawan Subedi, E Oniya, George S Polymeris, Dimitrios Afouxenidis, Nestor C Tsirliganis, and George Kitis. Thermal quenching of thermoluminescence in quartz samples of various origin. *Nuclear Instruments and Methods in Physics Research Section B: Beam Interactions with Materials and Atoms*, 269(6):572–581, 2011.
 143. C M Sunta, W E F Ayta, J F D Chubaci, and S Watanabe. A critical look at the kinetic models of thermoluminescence: I. first-order kinetics. *Journal of Physics D: Applied Physics*, 34(17):2690–2698, aug 2001.
 144. C M Sunta, W E F Ayta, J F D Chubaci, and S Watanabe. A critical look at the kinetic models of thermoluminescence II. non-first order kinetics. *Journal of Physics D: Applied Physics*, 38(1):95–102, dec 2004.
 145. M Tachiya and A Mozumder. Decay of trapped electrons by tunnelling to scavenger molecules in low-temperature glasses. *Chemical Physics Letters*, 28(1):87 – 89, 1974.
 146. P Thioulouse, E A Giess, and I F Chang. Investigation of thermally stimulated luminescence and its description by a tunneling model. *Journal of Applied Physics*, 53(12):9015–9020, 1982.
 147. A Timar-Gabor, D Constantin, J P Buylaert, M Jain, A S Murray, and A G Wintle. Fundamental investigations of natural and laboratory generated SAR dose response curves for quartz OSL in the high dose range. *Radiation Measurements*, 81:150 – 156, 2015.
 148. A Timar-Gabor, A Vasiliniuc, D A G Vandenberghe, C Cosma, and A G Wintle. Investigations into the reliability of SAR-OSL equivalent doses obtained for quartz samples displaying dose response curves with more than one component. *Radiation Measurements*, 47(9):740 – 745, 2012.
 149. F Trompier, C Bassinet, S Della Monaca, A Romanyukha, R Reyes, and I Clairand. Overview of physical and biophysical techniques for accident dosimetry. *Radiation Protection Dosimetry*, 144:571–574, March 2011.
 150. S. Tsukamoto, P.M. Denby, A.S. Murray, and L. Bøetter-Jensen. Time-resolved luminescence from feldspars: New insight into fading. *Radiation Measurements*, 41(7):790 – 795, 2006.
 151. D A G Vandenberghe, M Jain, and A S Murray. Equivalent dose determination using a quartz isothermal TL signal. *Radiation Measurements*, 44(5):439 – 444, 2009.

152. R Visocekas. Tunneling radiative recombination in K-feldspar sanidine. *Nuclear Tracks and Radiation Measurements*, 21:175–178, 1993.
153. R Visocekas. Tunnelling in afterglow: its coexistence and interweaving with thermally stimulated luminescence. *Radiation Protection Dosimetry*, 100:45–53, 2002.
154. R Visocekas, V Tale, A Zink, and I Tale. Trap spectroscopy and tunnelling luminescence in feldspars. *Radiation Measurements*, 29:427–434, 1998.
155. Raphael Visocekas, T. Ceva, C. Martí, Françoise Lefaucheur, and M. C. Robert. Tunneling processes in afterglow of calcite. *Physica Status Solidi (a)*, 35:315–327, 1976.
156. M P R Wáligorski and R Katz. Supralinearity of peak 5 and peak 6 in TLD-700. *Nuclear Instruments and Methods*, 172(3):463 – 470, 1980.
157. M P R Wáligorski, P Olko, P Bilski, M Budzanowski, and T Niewiadomski. Dosemetric Characteristics of LiF:Mg,Cu,P Phosphors - A Track Structure Interpretation. *Radiation Protection Dosimetry*, 47(1-4):53–58, 05 1993.
158. A Wieser, Y Göksu, D F Regulla, and A Waibel. Unexpected superlinear dose dependence of the E1' centre in fused silica. *International Journal of Radiation Applications and Instrumentation. Part D. Nuclear Tracks and Radiation Measurements*, 18(1):175 – 178, 1991.
159. X H Yang and S W S McKeever. The pre-dose effect in crystalline quartz. *Journal of Physics D: Applied Physics*, 23(2):237, 1990.
160. D Yossian and Y S Horowitz. Mixed-order and general-order kinetics applied to synthetic glow peaks and to peak 5 in LiF:Mg, Ti (TLD-100). *Radiation Measurements*, 27(3):465 – 471, 1997.
161. E G Yukihara and S W S McKeever. Optically stimulated luminescence. Wiley, 2011.
162. E G Yukihara, V H Whitley, J C Polf, D M Klein, S W S McKeever, A E Akselrod, and M S Akselrod. The effects of deep trap population on the thermoluminescence of Al₂O₃:C. *Radiation Measurements*, 37(6):627 – 638, 2003.
163. J Zimmerman. The radiation-induced increase of the 100 °C thermoluminescence sensitivity of fired quartz. *Journal of Physics C: Solid State Physics*, 4(18):3265–3276, 1971.